ELSEVIER

Journal of Power Sources 77 (1999) 17–27

JOURNAL OF POWER SOURCES

Composition and performance modelling of catalyst layer in a proton exchange membrane fuel cell

Curtis Marr, Xianguo Li *

Department of Mechanical Engineering, University of Victoria, Victoria, British Columbia, Canada V8W 3P6

Received 15 September 1997; revised 24 August 1998; accepted 5 September 1998

Abstract

The composition and performance optimisation of cathode catalyst platinum and catalyst layer structure in a proton exchange membrane fuel cell has been investigated by including both electrochemical reaction and mass transport process. It is found that electrochemical reactions occur in a thin layer within a few micrometers thick, indicating ineffective catalyst utilization for the present catalyst layer design. The effective use of platinum catalyst decreases with increasing current density, hence lower loadings of platinum are feasible for higher current densities of practical interest without adverse effect on cell performance. The optimal void fraction for the catalyst layer is about 60% and fairly independent of current density, and a 40% supported platinum catalyst yields the best performance amongst various supported catalysts investigated. An optimal amount of membrane content in the void region of the catalyst layer exists for minimum cathode voltage losses due to competition between proton migration through the membrane and oxygen transfer in the void region. The present results will be useful for practical fuel cell designs.

Keywords: PEM fuel cell; Catalyst layer; Optimization

1. Introduction

Vehicular emissions arising from fossil fuel combustion have resulted in severe local air pollution in many urban areas. They causes health problems, and contributes significantly to the accumulation of atmospheric greenhouse gases with possible detrimental changes in the global climate. The increasing consumption of finite fossil fuel reserves has also called for alternative fuels and energy sources for sustainable development. Proton exchange membrane fuel cells (PEMFC), using hydrogen as fuel, are promising candidates for transportation applications as a clean and energy efficient power source.

However, the commercial success of PEMFCs depends on their cost competitiveness with other energy conversion and power generation devices. Cost reduction of PEM fuel cells can be achieved by enhancing performance (high energy conversion efficiency and power density) and lowering material and fabrication costs. In PEMFCs, the conversion of the chemical energy of a fuel and an oxidant into electricity is accomplished in a thin layer of catalyst located between the membrane electrolyte and cathode, and the electrolyte and anode, often referred to as the cathode and anode catalyst layer, respectively. Due to the low cell operating temperature (80–95°C) and acidic nature of the reaction, expensive precious metals like platinum and its alloys are invariably used as catalyst to facilitate the electrochemical reactions. If PEMFCs are successful in replacing the present internal combustion engines as the vehicle power source, substantial increases in world platinum production will be required at the present loadings of platinum.

An estimate of required platinum production may be made as follows: assume each vehicle has a power source of 50 kW net power, provided by PEMFCs with a power density of 0.6 W/cm^2 and a cell platinum loading of 1 mg/cm^2. Then each new vehicle power train requires 83.3 g of platinum. Considering approximately 2.2 g of platinum per vehicle [1] is currently expected to be used for

* Corresponding author. Department of Mechanical Engineering, Faculty of Engineering, 200 University Avenue West, University of Waterloo, Waterloo, Ontario, Canada N2L 3G1. Tel.: 1+519-888-4567; Fax: 1-519-888-6197

0378-7753/99/$19.00
PII: S0378-7753(98)00161-X

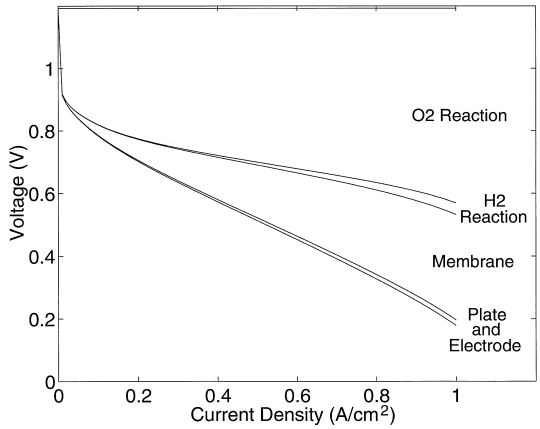

Fig. 1. Typical breakdown of cell voltage losses in a proton exchange membrane fuel cell [4].

spark plugs and catalytic converters, and 16 million new vehicles produced per year in North America [2], a 95% recovery rate from platinum recycling requires an additional 31.5 tonnes of platinum production per year. This dictates an increase of 22% in world annual platinum production, which is approximately 144 tonnes/year [3], in order to maintain new vehicle production in North America alone. However, before large scale market penetration of fuel cells into transportation applications, platinum recycling is not available and economically viable. On the other hand, if PEM fuel cells successfully becomes the choice of power source for the 2% zero emission vehicles, required by year 2003, out of total 16 million new vehicles produced annually, that requires an increase of 26 tonnes, or 18%, beyond the current world annual platinum production solely for the North American market. Therefore, minimisation of platinum usage in PEMFCs is of significance not only in the reduction of PEMFC intrinsic cost, but also to mitigate rises in platinum cost from increased demand.

Because the thin catalyst layers are the regions where the electric power is generated, cell performance depends largely on the optimisation of various processes occurring there. As shown in Fig. 1, the highest irreversible losses in cell voltage occur in the cathode catalyst layer at practical current densities of 0.3–0.5 A/cm^2, while the losses in the anode catalyst layer are relatively small by comparison [4]. Hence, performance of the cathode catalyst layer in a PEMFC has significant impact on the overall performance of the cell, and the optimisation of cathode catalyst layer composition and performance becomes the objective of the present study.

Previous studies have concentrated on various aspects of PEMFC operation, and their effect on cell performance. Fuller and Newman [5] investigated strategies for thermal and water management. Springer et al. [6] developed an isothermal, one-dimensional, steady state model for water transport through a complete PEMFC based on experimental results, and their modelling results provided useful insight into the cell's water transport mechanisms and their effect on the cell performance. Bernardi and Verbrugge [7,8] developed a comprehensive mathematical model for a PEMFC from fundamental transport properties. Nguyen and White [9] formulated a quasi-two-dimensional model to account for the variations of mass and heat transfer between the electrode and reactant gas mixture in the flow channel. Amphlett et al. [10] presented a semi-empirical model for a specific PEMFC performance. Recently, Weisbrod et al. [11] presented a simplified through-the-electrode model, including water saturation and transport within the electrode and reaction kinetics within the cathode catalyst layer. The model was validated with single cell experimental data, and was then used to investigate the impact of cell operating temperature and pressure on the cell performance.

Clearly, few studies in literature have focused on the catalyst layer performance and its composition optimisation under various conditions, as well as the impact on cell performance. The present study follows earlier work of Bernardi and Verbrugge [7,8], and Weisbrod et al. [11]. A steady state, isothermal and one-dimensional model of the cathode catalyst layer is formulated by including both electrochemical kinetics and mass transport processes of reactant oxygen dissolved in a fully hydrated ionomer membrane. The present results highlight the existence of optimal operating and design parameters as well as their inter-dependence, and will be useful in aiding the design of practical fuel cells.

2. Formulation

The cathode catalyst layer is assumed to consist of a mixture of catalyst platinum, ionomer membrane electrolyte and void space, as shown schematically in Fig. 2.

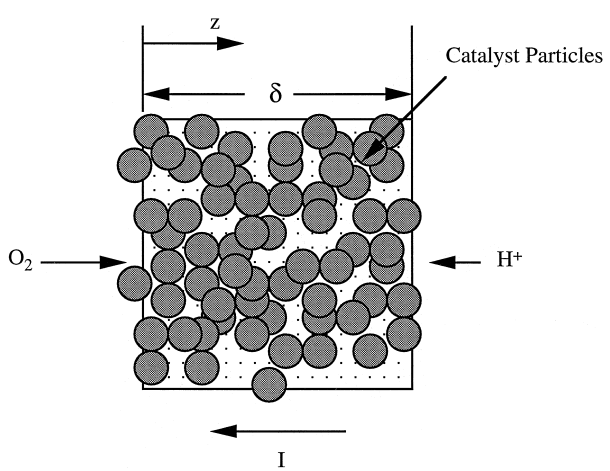

Fig. 2. Schematic of the cathode catalyst layer.

The small catalyst particles, either on their own or supported on relatively large carbon black particles, are covered by a thin, continuous layer of ionomer. The spatial coordinate z is defined in Fig. 2 so that the positive direction points from the cathode electrode to the membrane with its origin located at the interface between the cathode electrode and catalyst layer. All fluxes are taken as positive in the positive z-direction, while the electric current density is opposite to the z-direction, as shown. The void space is usually sufficiently large so that the Knudsen diffusion is unimportant compared to the bulk diffusion [12]. It is further assumed that the catalyst layer has a uniform distribution of its various components and a small thickness compared to its height and depth so that a one-dimensional approximation in the z-direction is made.

In the catalyst layer, protons diffuse into the layer from the anode through the membrane on the right and oxygen diffuses into the layer from the cathode electrode on the left. Electrons from the electrode travel through either the catalysed carbon black particles or platinum particles, depending on the type of catalyst used, to the catalyst surface. On the surface of the catalyst particles, the oxygen is consumed along with the protons and electrons and the product liquid water is produced along with the waste heat. The overall electrochemical reactions occurring at the reaction site may be represented by the following reaction:

$$4H^+ + 4e^- + O_2 \rightarrow 2H_2O + \text{Heat} \quad (1)$$

The liquid water formed at the catalyst surface may be removed through the cathode electrode or via back diffusion through the membrane to the anode, depending on the operating condition. Therefore, the ionomer layer surrounding the catalyst particles is taken to be fully hydrated, and the void region in the catalyst layer is assumed to be fully flooded, although many other researchers have assumed open gas pores in their modelling of single cell performance [5–11]. This is because in many of the single cell experimental measurements based on which these previous models were developed, water flooding is not a serious problem at reasonable current densities, especially under relatively high stoichiometric flow rates of the reactants used in those studies in order to boost cell performance. In fact, entire reaction product—liquid water—can be removed from the anode side to avoid water flooding of the cathode if sufficiently high fuel stream flow rates are employed [13,14]. On the other hand, there are experimental evidences that water flooding occurs at very low current densities during the operation of practical fuel cell stacks because the stoichiometric flow rates of the reactants involved cannot be excessively high due to, e.g., efficiency and economic consideration and practical limitations. Since a stack or stacks of many individual cells have to be put together for all practical applications, and the purpose of the present study is to provide aids for practical fuel cell designs, it is justifiable to assume that the cathode catalyst layer is fully flooded. Ideally, one might like to study the case of partially-flooded cathode, and to investigate the effect of the various degree of water flooding on the performance and optimal design—this is not an easy problem, and it will be dealt with in a future study. The waste heat produced may be removed in a manner similar to that of water removal such that the entire catalyst layer maintains isothermal conditions. As a result, the primary processes to be modelled in the catalyst layer are electrochemical reactions at the catalyst surface as given in Eq. (1), the delivery of reactants to the reaction site and the ohmic losses associated with proton and electron migration.

The reactant supply to the reaction site is governed by the conservation of species. For an infinitesimal control volume $\mathrm{d}z$ located at z, this becomes

$$\frac{\mathrm{d}C_i}{\mathrm{d}t} = -\frac{\mathrm{d}N_i}{\mathrm{d}z} + \omega_i \quad (2)$$

where C_i is the molar concentration of species i, N_i is the molar flux, and ω_i is the rate of production for species i due to the electrochemical reaction. At steady state, no species accumulation occurs within the control volume, thus Eq. (2) reduces to, for the three reactant species,

$$\frac{\mathrm{d}N_{O_2}}{\mathrm{d}z} = \omega_{O_2} \quad (3)$$

$$\frac{\mathrm{d}N_{H^+}}{\mathrm{d}z} = \omega_{H^+} \quad (4)$$

$$\frac{\mathrm{d}N_e}{\mathrm{d}z} = \omega_e \quad (5)$$

The rate of species production is related by the stoichiometric coefficients of the various species involved in the reaction. For the cathode reaction given in Eq. (1)

$$-\omega_{O_2} = -\frac{1}{4}\omega_{H^+} = -\frac{1}{4}\omega_e = \frac{1}{2}\omega_{H_2O} = \omega \quad (6)$$

where ω represents the rate of reaction.

Combining Eqs. (3), (4) and (6) yields

$$\frac{\mathrm{d}N_{O_2}}{\mathrm{d}z} = \frac{1}{4}\frac{\mathrm{d}N_{H^+}}{\mathrm{d}z} \quad (7)$$

Integrating from the membrane/catalyst layer interface to any location z in the catalyst layer, and noting that the proton molar flux and protonic electric current density are related by Faraday's constant ($F = 96{,}487$ coulombs/mol) with the relation $I = -N_{H^+}F$, where the negative sign arises from the fact that the positive direction of the current density I is opposite to the proton flux assumed, and the oxygen molar flux N_{O_2} vanishes at $z = \delta$ by assuming that no oxygen crosses through the membrane, we have

$$N_{O_2}(z) = -\frac{1}{4F}\left[I(z) - I_\delta\right] \quad (8)$$

where $I_\delta = I(\delta)$ represents the current density loading for the cell. The oxygen flux through the catalyst layer is assumed due to concentration gradient only, so that from the Fick's law of diffusion, we have

$$\frac{dC_{O_2}}{dz} = -\frac{N_{O_2}}{D_{O_2}^{eff}} \tag{9}$$

where the effective diffusion coefficient, $D_{O_2}^{eff}$, is calculated from the bulk diffusion coefficient, D_{O_2}, for oxygen diffusion through the void region of the catalyst layer and a correction factor to account for the non-diffusing space occupied by the solid catalyst particles [17]

$$D_{O_2}^{eff} = \phi^{3/2} D_{O_2} \tag{10}$$

where ϕ represents the void fraction, or porosity, of the catalyst layer. Combining Eqs. (8) and (9) gives the equation for the oxygen concentration variation in the catalyst layer

$$\frac{dC_{O_2}}{dz} = \frac{1}{4FD_{O_2}^{eff}}\left[I(z) - I_\delta\right] \tag{11}$$

As mentioned earlier, the void space in the catalyst layer is filled completely with a mixture of water and ionomer, and oxygen dissolved in liquid water diffuses through the liquid water first, then through the thin ionomer surrounding the catalyst particle before reaching the reaction sites. If the ionomer coating the catalyst is evenly distributed over the catalyst particles, the overall O_2 diffusion processes in the void region of the catalyst layer may be approximated with a series resistance model. At steady state, the resistance, per unit area, to O_2 transfer by diffusion is [18]

$$\frac{L_l + L_m}{D_{O_2}} = \frac{L_l}{D_{O_2\text{-}H_2O}} + \frac{L_m}{D_{O_2\text{-}m}} \tag{12}$$

where L_l and L_m are the equivalent thickness of liquid water and ionomer membrane, respectively, in the catalyst layer per unit geometrical surface area, and $D_{O_2\text{-}H_2O}$ and $D_{O_2\text{-}m}$ are the diffusion coefficient of O_2 in liquid water and membrane, respectively. Because the ionomer loading l_m of the catalyst layer is defined as the ratio of the volume occupied by the ionomer to the total void space available in the catalyst layer, it is directly proportional to the equivalent thickness L_m. Then, Eq. (12) can be rearranged to give the bulk O_2 diffusion coefficient as follows:

$$D_{O_2} = \frac{D_{O_2\text{-}m} D_{O_2\text{-}H_2O}}{(1 - l_m) D_{O_2\text{-}m} + l_m D_{O_2\text{-}H_2O}} \tag{13}$$

The ohmic resistance in the catalyst layer is associated with both proton migration through the ionomer and electron transfer in the conducting solid catalyst. Applying Ohm's law to both the proton and electron motion yields

$$\frac{d\psi_s}{dz} = -\frac{I_e}{\kappa_s^{eff}} \tag{14}$$

and

$$\frac{d\psi_m}{dz} = -\frac{I}{\kappa_m^{eff}} \tag{15}$$

where ψ_s and ψ_m represent electrical potential in the solid catalyst particles and ionomer membrane, respectively, κ_s and κ_m are the corresponding electrical conductivity, I_e denotes the electronic current density and I the protonic current density defined earlier. Because the overpotential η in the cathode layer driving the electrochemical reactions is related to the difference in potential ψ_s and ψ_m as follows:

$$\eta = \psi_s - \psi_m + \text{constant} \tag{16}$$

the change of η becomes, from Eqs. (14) and (15)

$$\frac{d\eta}{dz} = -\frac{I_e}{\kappa_s^{eff}} + \frac{I}{\kappa_m^{eff}} \tag{17}$$

The electronic and protonic current density can be related. From Eqs. (4)–(6), we have $dI/dz = -dI_e/dz$ because both the protonic and electronic current density are proportional to their respective molar flux. Integrating from δ to z yields

$$I(z) - I(\delta) = -I_e(z) \tag{18}$$

since $I_e(\delta) = 0$ as the membrane region is electronically insulated, no electrons can flow through the membrane. Substitution of Eq. (18) into Eq. (17) results in

$$\frac{d\eta}{dz} = \left(\frac{1}{\kappa_m^{eff}} + \frac{1}{\kappa_s^{eff}}\right) I - \frac{1}{\kappa_s^{eff}} I_\delta \tag{19}$$

Typically, the electrical conductivity in the solid is several orders of magnitude larger than that in the ionomer so that the second term in the above equation is almost always small relative to the first term, except for very small current densities near $z = 0$. The effective electric and ionic conductivity are determined from the correlations accounting for the porous nature of the catalyst layer [17] similar to that for gas diffusion discussed earlier. They are

$$\kappa_m^{eff} = (l_m \phi)^{3/2} \kappa_m \tag{20}$$

$$\kappa_s^{eff} = (1 - \phi)^{3/2} \kappa_s \tag{21}$$

where κ_m and κ_s are the bulk conductivities of the ionomer and solid catalyst, respectively. In obtaining Eq. (20), it has been assumed that the liquid water in the void

region of the catalyst layer blocks the conduction of proton in a similar non-linear fashion as solid spheres.

The distribution of the current density $I(z)$ within the catalyst layer, as appeared in Eqs. (11) and (19), depends on the rate of electrochemical reaction ω shown in Eq. (6). For fully hydrated ionomer in the cathode catalyst layer, the concentration of proton at the reaction sites is fixed and constant, and its specific value depends on the type of the membrane used. Therefore, absorbing the proton concentration into the pre-exponential constant, which eventually becomes the exchange current density, the Butler–Volmer equation for the rate of the electrochemical reaction given in Eq. (1) becomes

$$\omega* = B* C_{O_2}^{\gamma}\left[\exp\left(\frac{\alpha_c F\eta}{RT}\right) - \exp\left(-\frac{\alpha_a F\eta}{RT}\right)\right] \quad (22)$$

where α is the transfer coefficient, η is the cathode overpotential, T is the temperature of the catalyst layer, R is the universal gas constant, and $B*$ is the pre-exponential constant. Typically, the reaction order γ is usually taken as unity. The reaction rate $\omega*$ represents the molar change per unit time per unit reaction surface area. It should be pointed out that oxygen reduction in acidic media is in general irreversible like in the phosphoric acid fuel cells (PAFCs), and the open-circuit potential (i.e., at zero cell current density) is a mixed potential between some electrode oxidation process, such as carbon oxidation and oxygen reduction. Therefore, high cell voltage operation must be avoided for PAFCs in order to extend cell lifetime [15]. However, for PEM fuel cells which operate at much lower temperature (about 80°C) than the corresponding phosphoric acid fuel cells (about 200°C), experimental observations [15] indicate that the electrode corrosion reactions, typically occurring at open-circuit voltage or at extremely small cell current densities, are much alleviated compared to the PAFCs. Further, all practical PEM fuel cells operate at current densities far away from the open-circuit voltage in order to maximize cell power output, and at such practical cell current densities (>0.1 A/cm^2) the electrode corrosion reactions are negligible. Therefore, almost all the past PEM fuel cell models have adopted the Butler–Volmer equation for the electrochemical reactions, and the model results agree reasonably well with various experimental results (e.g., see Refs. [5–11,16]).

Because the catalyst layer is not flat, but composed of a mixture of three-dimensional particles, the surface reaction rate $\omega*$ can be converted into a volumetric reaction rate ω by the effective catalyst surface area per unit geometric volume of the catalyst layer, A_v, through the relation $\omega = \omega* A_v$. Combining with Eqs. (4) and (6) and noting that $I = -N_{H^+}F$, we have

$$\frac{dI}{dz} = A_v B C_{O_2}^{\gamma}\left[\exp\left(\frac{\alpha_c F\eta}{RT}\right) - \exp\left(-\frac{\alpha_a F\eta}{RT}\right)\right] \quad (23)$$

where $B = 4FB*$ is a constant, usually determined from a reference value measured at a known reference oxygen concentration at the reaction site, i.e.,

$$B = i_{0,ref}/C_{O_2,ref}^{\gamma} \quad (24)$$

Then the current density distribution, Eq. (23), becomes

$$\frac{dI}{dz} = A_v i_{0,ref}\left(\frac{C_{O_2}}{C_{O_2,ref}}\right)^{\gamma}\left[\exp\left(\frac{\alpha_c F\eta}{RT}\right) - \exp\left(-\frac{\alpha_a F\eta}{RT}\right)\right] \quad (25)$$

The specific reaction surface area A_v is given by

$$A_v = m_{Pt} A_s/\delta \quad (26)$$

where m_{Pt} is the catalyst mass loading per unit area of the cathode, A_s is the catalyst surface area per unit mass of the catalyst, and δ is the catalyst layer thickness. The catalyst surface area varies greatly for different types of supported catalysts and platinum black, as shown in Table 1 [19].

It should be noted that the void fraction ϕ is related to the type of catalyst, m_{Pt} and δ as follows:

$$\phi = 1 - \left(\frac{1}{\rho_{Pt}} + \frac{1 - \%Pt}{\%Pt\,\rho_C}\right)\frac{m_{Pt}}{\delta} \quad (27)$$

where %Pt represents the percentage of platinum catalyst on the carbon black support by mass, ρ_{Pt} and ρ_C are the densities of platinum and carbon black, respectively. Therefore, for a given type of catalyst, only two out of the three parameters (ϕ, m_{Pt} and δ) need to be specified and the third can be determined from Eq. (27). For pure platinum, often called platinum black, %Pt = 100%. It should be noted that the true volume density of carbon black may be higher than the density of the packed carbon powder materials, and the effective density of a platinum/carbon layer may vary, depending on, e.g., the method of preparation and fabrication. However, the difference in these various densities is represented in the present model by the void fraction as defined in Eq. (27). The void fraction is a macroscopic parameter representing the porous nature of the catalyst layer, although the microscopic characteristics of the layer may be very complex and difficult to describe exactly.

Table 1
Representative catalyst surface areas for different catalyst types [19]

Catalyst type	Surface area/Pt mass, A_s (m^2/g)
10% Pt on carbon black	140
20% Pt on carbon black	112
30% Pt on carbon black	88
40% Pt on carbon black	72
60% Pt on carbon black	32
80% Pt on carbon black	11
Pt black	28

The experimental data of Parthasarathy et al. [20] were used to correlate the reference exchange current density for oxygen reduction in Nafion. The data were correlated with the cell temperature, with a confidence level of 97.7%

$$\log_{10}(i_{0,\mathrm{ref}}) = 3.507 - \frac{4001}{T} \quad (28)$$

where $i_{0,\mathrm{ref}}$ is in A/cm^2 and temperature T is in Kelvins.

Because the model Eqs. (11), (19) and (25) consist of three first order ordinary differential equations, three boundary conditions are required for a unique solution. At the cathode electrode and catalyst layer interface, the protonic current must vanish as electrode is ionically insulated:

$$I = 0 \text{ at } z = 0 \quad (29)$$

On the other hand, the protonic current density at $z = \delta$ is equal to the cell current density, or

$$I = I_\delta \; at \, z = \delta \quad (30)$$

The oxygen concentration at $z = 0$ is taken to be known. There oxygen gas dissolves into the liquid water before transporting into the fully flooded catalyst layer. Hence, $C_{O_2}(0)$ is determined instead of arbitrarily specified, from the solubility of oxygen gas in liquid water using the Henry's law:

$$C_{O_2}(0) = \frac{p_{O_2}}{H_{O_2}} \text{ at } z = 0 \quad (31)$$

where $C_{O_2}(0)$ is the oxygen concentration in the liquid water at $z = 0$, p_{O_2} is the partial pressure in atm of oxygen on the gas side, and H_{O_2} is the Henry's constant for oxygen gas dissolution in liquid water (atm cm^3/mol). The Henry's constant is calculated from an empirical correlation [8]

$$\ln(H_{O_2}) = -\frac{666}{T} + 14.1 \quad (32)$$

3. Operating conditions and physical parameters

There are several operating and physical parameters that are needed for the model calculations. In this study, it is assumed that the oxygen from the cathode flow channel diffuses through the unflooded electrode void region. The diffusion through the electrode is modelled using a Bruggeman correction factor to account for the effect of void fraction [10]. A similar approach is used for the fuel transport in the anode side. Both electrodes are assumed with a thickness of 0.30 mm and void fraction of 0.40. Further, an operating pressure of 3 atm and temperature of 350 K is used with a stoichiometry of 2.0 and a fully saturated gas stream of 20%/80% O_2/N_2 for the cathode reactant and of pure H_2 for the anode reactant. Tables 2 and 3 summarise the parameters used in the present model calculations. A complete description of the conditions and methodology used can be found in Ref. [4]. It should be noted that in Table 3 the diffusion coefficient for oxygen in liquid water is obtained from the Wilke–Chang equation [21], and the diffusion coefficient (cm^2/s) for oxygen in Nafion is calculated using an empirical relation derived from a curve fit of data published in Ref. [20]:

$$D_{O_2-m} = -1.0664 \times 10^{-5} + 9.0215 \times 10^{-6} \times \exp\left(\frac{T - 273.15}{106.65}\right) \quad (33)$$

Table 2
Operating parameters used in the present model calculations

Parameter	Value
Cell inlet pressure	3 atm abs
Cell temperature	350 K
Cathode gas mixture	20%/80% O_2/N_2
Relative humidity	100%
O_2 stoichiometry	2.0
Anode gas mixture	100% H_2
Relative humidity	100%
H_2 stoichiometry	2.0

Table 3
Physical parameters used in the present model calculations

Parameter	Value
α_c	1.0
α_a	0.5
$D_{O_2\text{-}H_2O}$	9.19×10^{-5} cm^2/s
$D_{O_2\text{-}m}$	7.88×10^{-6} cm^2/s
κ_s	7.27×10^{2} S/cm
κ_m	0.170 S/cm
ρ_C	2.0 g/cm^3
ρ_{Pt}	21.5 g/cm^3
$C_{O_2,\mathrm{ref}}$	1.2×10^{-6} mol/cm^3

4. Results and discussion

A fourth order Runge–Kutta method [22] is used to solve the set of governing differential equations, and Fig. 3 shows a typical result for the distribution of the O_2 concentration, current density and cathode overpotential within the cathode catalyst layer. The layer considered has a thickness of 5.0 μm and a platinum loading of 4.0 mg/cm^2 and is operated at the conditions listed in Tables 2 and 3. The cell current density for this figure is 0.5 A/cm^2. The current density $I(z)$ has been normalised by I_δ, while the O_2 concentration and overpotential are normalised by their respective values at $z = 0$, $C_{O_2}(0) = 0.7 \times 10^{-6}$ mol/cm^3 and $\eta(0) = 0.567$ V. It is seen from the figure that the O_2 concentration decreases rapidly whereas the current den-

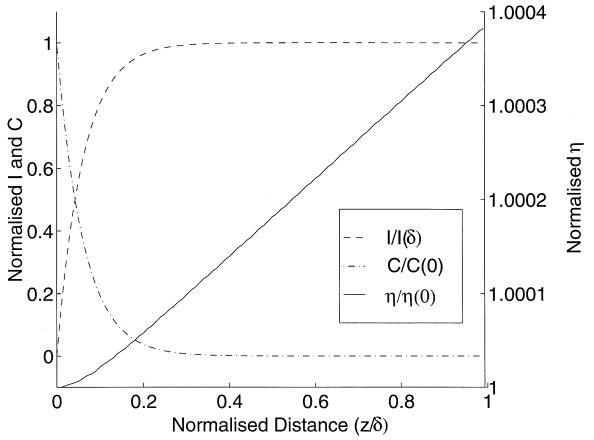

Fig. 3. Distribution of current density, O_2 concentration and overpotential in the catalyst layer of 5 μm thick for 0.5 A/cm^2 and 4 mg/cm^2 Pt black loading.

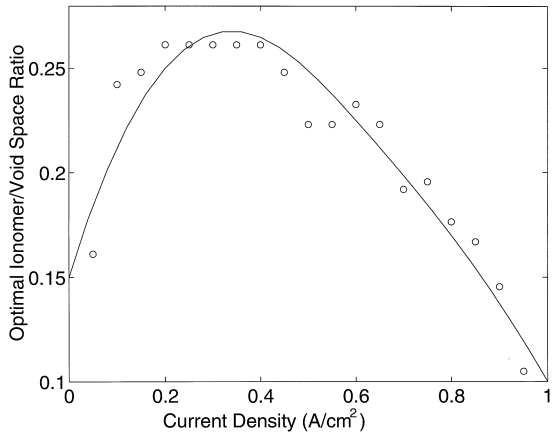

Fig. 5. Optimal ionomer loading as a function of the cell current density for a 5.0 μm thick layer of Pt black and a platinum loading of 4 mg/cm^2.

sity increases nearly exponentially. At a distance less than 40% of the catalyst layer thickness, the O_2 concentration vanishes while the current density reaches the value of I_δ. In fact, within the first 20% of the catalyst layer thickness, over 95% of the O_2 has been consumed by the electrochemical reaction for the production of electric current, and consequently very little of the reaction occurs in the remainder of the catalyst layer. Therefore, the cathode overpotential $\eta(z)$ is nearly linear with z for the majority of the layer, except for $z/\delta < 20\%$, where η increases more slowly. It should also be pointed out that the variation of η is quite small within the catalyst layer (less than 0.1%) as compared with the O_2 concentration and the current density.

The cathode overpotential, as pointed out earlier, constitutes the largest irreversible losses in the cell voltage, and is influenced by the composition of the void space in the catalyst layer. Because the diffusion of oxygen is faster through liquid water than ionomer, increased oxygen concentration will result from decreasing the amount of ionomer in the void space l_m. Conversely, increasing the ionomer loading in the void space will increase the ionic conductivity and lower the ohmic resistance to proton migration. In Fig. 4, the volume of the void space occupied by ionomer, l_m, is varied from 5% to 100% of the void space for current densities from 0.05 to 0.6 A/cm^2 at the operating conditions specified in the previous section. For the calculations, a 5 μm thick layer of Pt black is used with a platinum loading of 4 mg/cm^2. It is seen that the cathodic overpotential decreases first as ionomer content is increased, due to increased ionic conductivity for proton transfer. However, the resistance to O_2 transport is increased at the same time, and becomes dominant at higher ionomer loadings, leading to an increase in the voltage loss. It is also clear that the overpotential increases significantly with the cell current density, and the minimum voltage loss and the corresponding optimal ionomer loading depend on the cell current density as well.

The optimal ionomer loading has been determined by using a Golden Section algorithm [23] and the results are

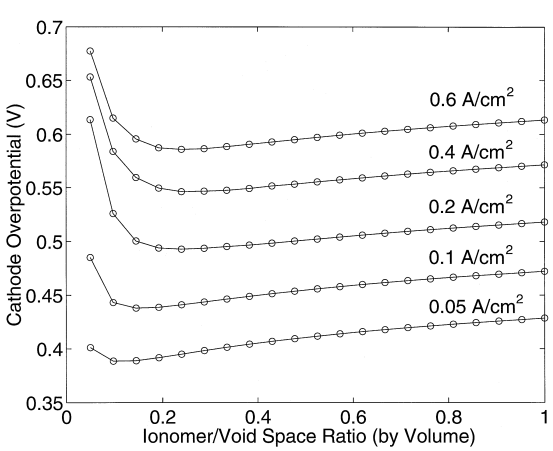

Fig. 4. Effect of ionomer content in the void region of the catalyst layer on overpotential for a 5.0 μm thick layer of Pt black with a platinum loading of 4 mg/cm^2.

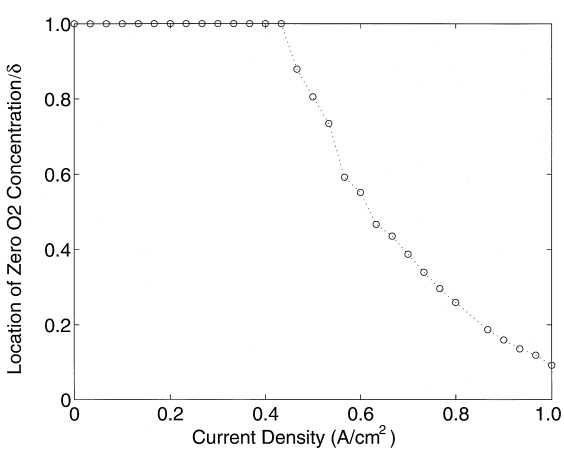

Fig. 6. Location of zero O_2 concentration in the catalyst layer, normalized by the layer thickness δ, as a function of cell current density for 4 mg/cm^2 Pt black loading and 5 μm layer thickness.

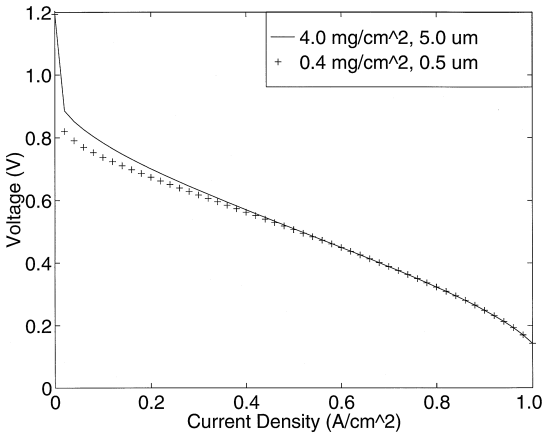

Fig. 7. Effect on cell performance of reducing both Pt loading and catalyst layer thickness by a factor of 10. Catalyst used is platinum black.

shown in Fig. 5 as a function of the cell current density. The apparent scatter in the calculated data points is due to the relatively small changes in the overpotential for different ionomer loadings, and truncation errors in the numerical solution. It is evident that the optimal ionomer loading increases with the cell current density I_δ until reaching a maximum value around $I_\delta = 0.3$ A/cm^2, then it decreases at higher current densities. The point of decrease starts in the range of current densities where mass transport limitations begin to occur. This behaviour of the optimal ionomer loading l_m can be explained physically as follows: at low I_δ the rate of O_2 diffusion is sufficiently fast compared to the rate of electrochemical reactions, as a result, higher ionomer loading reduces voltage losses associated with proton transfer. On the other hand, high cell current densities consume a large quantity of reactants, making oxygen supply the controlling process for optimal performance. Hence a decrease in the ionomer loading is required for a larger passage for faster mass transfer of the reactant oxygen.

The rapid decrease of the O_2 concentration in the catalyst layer, as shown in Fig. 3, is due to the finite rate of mass transfer and fast consumption by the electrochemical reactions. As a result, not all the expensive catalyst in the layer is used for the production of electricity. This implies that the portion of unused catalyst can be removed without any effect or degradation of the catalyst layer performance. The portion of the catalyst that contributes to the electrochemical reaction is indicated by the location of zero O_2 concentration. Note that the location of zero O_2 concentration corresponds to the location where $I(z) = I_\delta$. Fig. 6 shows the location of zero O_2 concentration in the catalyst layer as a function of the cell current density I_δ for $\delta = 5$ μm and a platinum loading of 4.0 mg/cm^2. It is seen that for low current densities, the entire catalyst layer is used for electric current production. This is because the rate of O_2 consumption by the reaction is slow compared to the rate of mass transport, and O_2 has sufficient ability to diffuse into the entire catalyst layer. However, at the high cell current densities, the rate of O_2 consumption becomes very large by comparison, and O_2 concentration is quickly depleted before reaching out to the rest of the catalyst layer. Hence, due to the mass transport limitations, the use of the catalyst in the layer decreases as the cell current density loading is increased. The foregoing result

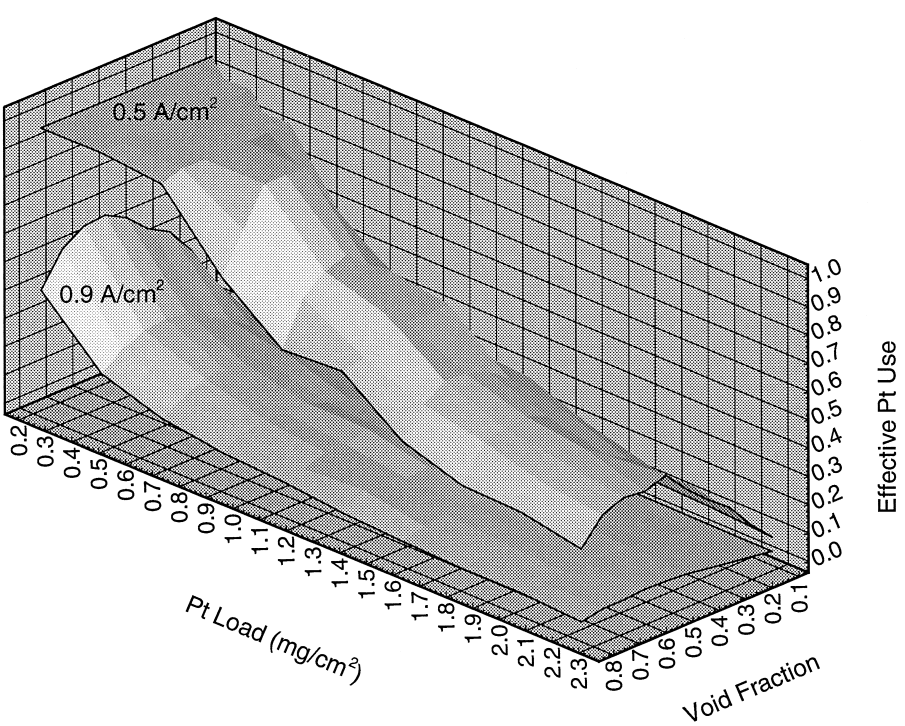

Fig. 8. Effect of Pt loading and void fraction on the effective Pt use for the current densities of 0.5 and 0.9 A/cm^2. Catalyst used is platinum black.

suggests that less catalyst is actually required at the practical high cell current densities than at the low cell current densities, opposite to common intuition. Therefore, a reduction of the platinum loading will not affect the catalyst layer performance at the practically high current densities, although the performance is somewhat lower at low values of I_δ. Fig. 7 illustrates the effect on the cell performance when both the platinum loading and the catalyst layer thickness are reduced by a factor of 10 [4]. Clearly, the cell performance is affected only at low I_δ. At high I_δ values of practical importance, the cell performance remains unchanged. This observation is of significant practical importance. First, the usual practice has been trying to achieve the cell polarisation curve as high as possible by increasing the platinum loading. This approach only increases the cell voltage at low current densities. Second, the energy conversion efficiency is proportional to the cell voltage, hence it increases as the cell current density I_δ is lowered (i.e., at partial load). However, the efficiency for almost all heat engines reduces at the partial load. Therefore, in order to compare the performance and cost of fuel cells with heat engines, fuel cells should be optimised at the designed operating conditions of high current density at which cell platinum loading can be safely reduced considerably from the present platinum loading level without degradation of cell performance. Although the fuel cell performance at the partial load is slightly decreased from its best possible condition, it will still be better than the corresponding heat engines. This approach would allow fuel cells with optimal performance and lower possible cost of materials.

Another implication is for the anode catalyst layer. Because the exchange current density for hydrogen oxidation is several orders of magnitude larger than the oxygen reduction reaction, the reactant H_2 may not penetrate deeply into the catalyst layer. As a result, significant amounts of platinum may be reduced for the anode catalyst layer as compared to the cathode side, and the current practice of using the same amount of platinum loading for both anode and cathode may not be the optimal approach for cell design.

The location of zero O_2 concentration in the catalyst layer represents the degree of platinum used in the fuel cell. As shown in Fig. 6, it depends on the operating conditions and the catalyst layer composition, and is the result of the balance between the electrochemical reaction and mass transport. The former is affected by the effective reaction surface areas per unit volume, A_v, and the latter is influenced by the void fraction, ϕ. For a given type of catalyst, A_v is related directly to the amount of platinum loading as given in Eq. (26). The catalyst utilization in the catalyst layer may be measured by effective platinum use defined below:

$$\text{Effective Pt Use} = \frac{\text{Location of zero } O_2 \text{ concentration, z}}{\text{Thickness of catalyst layer, } \delta} \quad (34)$$

which also represents the ratio of the platinum contributing to the reactions to the total amount of platinum in the catalyst layer. Fig. 8 shows the effect of platinum loading

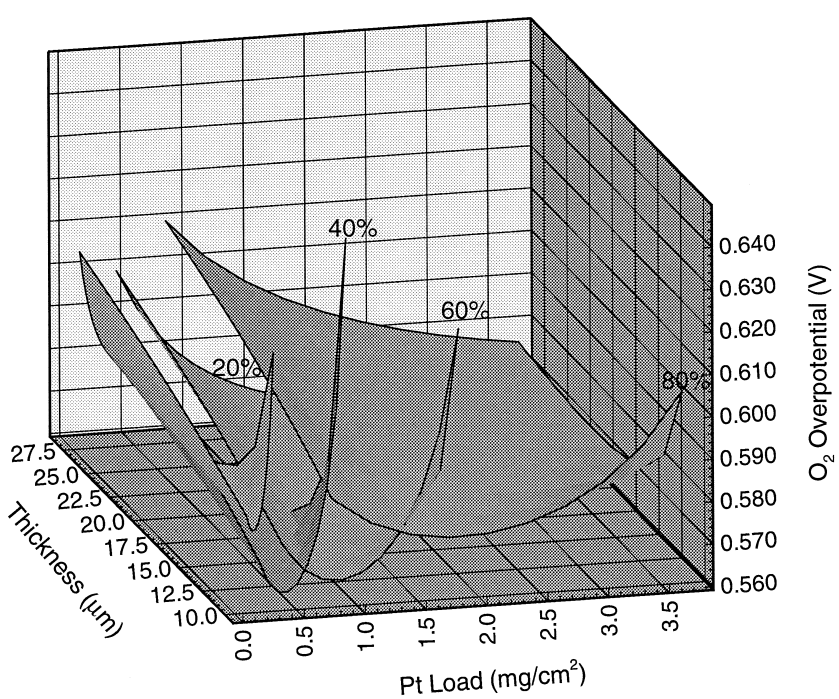

Fig. 9. Cathodic overpotential as a function of catalyst layer thickness, catalyst type and platinum loading at 0.5 A/cm^2. Percentage of platinum supported on carbon black is shown in the figure.

and void fraction on the effective platinum use for the current densities of 0.5 and 0.9 A/cm^2. The type of catalyst considered is platinum black. It is clear that the effective platinum use decreases significantly as the platinum loading and the cell current density are increased. There appears to exist an optimal void fraction of about 60%. At low void fraction, mass transport limitation keeps the platinum utilisation at a low level. An increase in the void fraction leads to more void space available for oxygen diffusion, contributing to higher platinum utilisation. However, the reaction surface area A_v is decreased, resulting in a thicker layer for a given platinum loading. Eventually the effective platinum use is reduced because the catalyst layer becomes too thick and the rate of mass transfer is limited.

The concept of effective platinum use yields lower optimal platinum loading, and is related to the reduction of cell material cost. However, conventionally platinum loading reduction has been achieved by increasing the effective reaction surface area through the use of small platinum particles supported on relatively large carbon black particles, as shown in Table 1. Fig. 9 shows the effect of supported catalyst on cathodic overpotential at the current density of 0.5 A/cm^2. It is seen that for a given catalyst there exists an optimal platinum loading, below which the shortage of reactive surface area increases the voltage loss. Above it, the voltage loss also increases due to the loss of void space for the oxygen supply for a given catalyst layer thickness.

For a given platinum loading, increase of the catalyst layer thickness also increases the voltage loss because of the limited rate of mass diffusion. For the same type of catalyst, it is also noticed that for high percentage platinum the voltage loss is less sensitive to the amount of platinum loading. Fig. 9 also reveals that there exists an optimal type of catalyst which yields the smallest cathodic voltage loss. Among the type of catalyst investigated, it is evident that 40% supported catalyst is the optimal one. Again, this is the result of trade-offs between the conflicting influence of the limited rate of mass transport and electrochemical reactions. As the percentage of platinum supported on carbon is reduced, the effective reactive surface area increases per unit mass of platinum. Therefore, the platinum loading is reduced. On the other hand, the lower percentage of supported catalyst eventually increases the voltage loss due to reduction in reaction surface area.

5. Conclusions

The performance of the cathode catalyst layer in a proton exchange membrane fuel cell (PEMFC) has been studied by including both electrochemical reaction and mass transport processes, and the composition and performance optimisation of catalyst platinum has also been investigated. It is found that most of the electrochemical reactions occurs in a thin layer within a few micrometers thick. This suggests that the catalyst is not being effectively utilised for the present catalyst layer design. It is also shown that the effective use of platinum catalyst decreases with increasing current density, and hence lower loadings of platinum are feasible for higher current densities of practical interest without adverse effect on cell performance. Further, it is possible to optimise the catalyst layer composition by considering the competing effects of increased reaction surface area and limited rate of reactant diffusion. It is shown that the optimal void fraction for the catalyst layer is about 60%, which appears to be fairly independent of current density, and a 40% supported platinum catalyst yields the best performance amongst 20%, 40%, 60% and 80% supported platinum catalysts investigated. There also exists an optimal amount of membrane content in the void region of the catalyst layer for minimum cathode voltage losses because of competition between proton migration through the ionomer membrane and oxygen transfer in the void region. The present results will be useful for the design of practical fuel cells.

Acknowledgements

This work was carried out as a part of a large CRD project supported by the Natural Sciences and Engineering Research Council of Canada (NSERC), British Gas and Ballard Power Systems. Partial financial support was also provided by a research grant from the NSERC.

References

[1] US Bureau of Mines, Minerals Yearbook, Vol. 1, 1992.
[2] S.G. Chalk, P.G. Patil, S.R. Venkateswaran, The new generation of vehicles: market opportunities for fuel cells, Journal of Power Sources 61 (1996) 7–13.
[3] Johnson-Matthey, Platinum 1995, 1995.
[4] C.L. Marr, Performance modelling of a single proton exchange membrane fuel cell, Master's thesis, University of Victoria, 1996.
[5] T.F. Fuller, J. Newman, Water and thermal management in solid polymer electrolyte fuel cells, J. Electrochem. Soc. 140 (5) (1993) 1218–1225.
[6] T.E. Springer, T.A. Zawodzinski, S. Gottesfeld, Polymer electrolyte fuel cell model, J. Electrochem. Soc. 138 (8) (1991) 2334–2342.
[7] D.M. Bernardi, M.W. Verbrugge, A mathematical model of a gas diffusion electrode bonded to a polymer electrolyte, AIChE 37 (9) (1991) 1151–1162.
[8] D.M. Bernardi, M.W. Verbrugge, A mathematical model of a solid polymer electrolyte fuel cell, J. Electrochem. Soc. 139 (9) (1992) 2477–2491.
[9] T.V. Nguyen, R.E. White, A water and heat management model for proton exchange membrane fuel cells, J. Electrochem. Soc. 140 (8) (1993) 2178–2186.
[10] J.C. Amphlett, R.M. Baumert, R.F. Mann, B.A. Peppley, P.R. Roberge, Performance modeling of the ballard mark IV solid polymer electrolyte fuel cell, J. Electrochem. Soc. 142 (1) (1995) 1–8.
[11] K.R. Weisbrod, S.A. Grot, N.E. Vanderborgh, Through-the-electrode model of a proton exchange membrane fuel cell, Electrochem. Soc. Proc. 23 (1995) 153–167.

[12] C.N. Satterfield, Mass Transfer in Heterogeneous Catalysis, MIT Press, Cambridge, 1970.
[13] H.H. Voss, D.P. Wilkinson, D.S. Watkins, Method and Apparatus for Removing Water from Electrochemical Fuel Cells, US Patent # 5260143, 1993.
[14] H.H. Voss, D.P. Wilkinson, P.G. Pickup, M.C. Johnson, V. Basura, Anode water removal: a water management and diagnostic technique for solid polymer fuel cells, Electrochimica Acta 40 (1995) 321–328.
[15] L.J.M.J. Blomen, M.N. Mugerwa, Fuel Cell Systems, Plenum, New York, 1993.
[16] T.E. Springer, M.S. Wilson, S. Gottesfeld, Modeling and experimental diagnostics in polymer electrolyte fuel cells, J. Electrochem. Soc. 140 (1993) 3513–3526.
[17] R.E. De la Rue, C.W. Tobias, On the conductivity of dispersions, J. Electrochem. Soc. 106 (1959) 827–833.
[18] M.N. Ozisik, Heat Transfer: A Basic Approach, McGraw-Hill, New York, 1985.
[19] E-TEK, Gas Diffusion Electrodes and Catalyst Materials, 1995 Catalogue, 1995.
[20] A. Parthasarathy, S. Srinivasan, J. Appleby, Temperature dependence of the electrode kinetics of oxygen reduction at the platinum/Nafion interface—a microelectrode investigation, J. Electrochem. Soc. 139 (9) (1992) 2530–2537.
[21] R.C. Reid, J.M. Prausnitz, T.K. Sherwood, The Properties of Liquids and Gases, McGraw-Hill, New York, 1977.
[22] W.H. Press, Numerical Recipes in C. Cambridge Univ. Press, New York, 1988.
[23] J.S. Arora, Introduction to Optimum Design, McGraw-Hill, New York, 1989.